

# Thermochemical Conversion of Lignocellulosic Biomass: a Thermodynamic Study Based on Isothermal and Adiabatic Reactors

Amanda C. C. Maia<sup>a</sup>, Julles M.Santos Júnior<sup>b</sup>, Annamaria D. S. Vidotti<sup>a</sup>, Antonio C. D. Freitas<sup>a</sup>, Reginaldo Guirardello<sup>b,\*</sup>

<sup>a</sup>Chemical Engineering Department, Exact Sciences and Technology Center, Federal University of Maranhão - UFMA, Av. dos Portugueses, 1966, Bacanga, 65080-805, São Luís-MA, Brazil

<sup>b</sup>School of Chemical Engineering, University of Campinas, Av. Albert Einstein 500, 13083-852, Campinas-SP, Brazil  
[guira@feq.unicamp.br](mailto:guira@feq.unicamp.br)

In this paper a comparative study is presented between thermochemical routes of pyrolysis (PR), Supercritical water gasification (SCWG), steam reforming (SR), oxidative reforming (OR) and autothermal reforming (ATR) aiming hydrogen production from lignocellulosic biomass (LB). For this, thermodynamic approaches were used, based on Gibbs energy minimization (*minG*) and entropy maximization (*maxS*) methods, in order to represent isothermal and adiabatic reactors, respectively. To carry out the simulations, the GAMS 23.9.5 software and the CONOPT3 solver were used. The results obtained demonstrated that the regions of greatest hydrogen formation were at high temperatures ( $\geq 900$  K) and at the lowest pressures tested (5 bar for PR; 230 bar for SCWG and 1 bar for the other thermochemical routes). Furthermore, it was verified which type of operation (adiabatic or isothermal) is most favourable for hydrogen production. The adiabatic operation proved to be more important and productive for SCWG and the isothermal operation proved to be efficient for all other thermochemical routes studied. It was also found that adiabatic reactors resulted in higher H<sub>2</sub> productivity for SR and PR processes; and isothermal reactors resulted in better quality of gas produced for the OR, ATR and SCWG processes. SR presented the best result for the quality of H<sub>2</sub> (47% in the product stream at 1 bar and 1000 K) produced. Exothermic reaction behaviours were observed for ATR, OR and for SCWG reactions, the other thermochemical routes presented endothermic characteristics in most of the operational ranges studied. The proposed thermodynamic models proved to be fast and effective in the calculations carried out in this paper, with computational times of less than 5 seconds in all performed simulations.

## 1. Introduction

Lignocellulosic biomass (LB) is an abundant and renewable resource from plants mainly composed of polysaccharides, cellulose and hemicelluloses and a polymer, the lignin. LB has a high potential as an alternative to fossil resources in order to produce second-generation biofuels and materials without compromising global food security. The modern biomass energy-conversion method includes thermochemical conversion and biochemical conversion routes for bioenergy production.

Different thermochemical routes are reported in literature to promote the conversion of biomass. Nanda et al. (2016) studied the subcritical and supercritical water gasification of lignocellulosic biomass with nickel nanocatalyst aiming hydrogen production, in this reaction, excess of water is used in a high-pressure reactor, high concentrations of hydrogen are reported in their results. In Zabaniotou et al. (2008) a study is carried out on the pyrolysis of lignocellulosic material, this reaction is conducted without the presence of other oxidizing agents in the system feed. Other routes that can be mentioned are steam reforming (biomass and water are fed to reactor), the partial oxidation reaction (atmospheric air or pure oxygen together with biomass are part of the reactor feed) and the autothermal reforming reaction (a direct combination of steam reforming and partial oxidation processes). Thermochemical routes are reported as robust and flexible, since it can be used for different types of residual materials (Arregi et al., 2018).

Understanding the thermal and reactional behavior of LB thermochemical transformation systems has not yet been completely elucidated, and within this scenario, thermodynamic analysis of these systems can contribute, elucidating the main aspects of the operational and thermal behavior of these systems during thermo chemical transformation. In this way, in this paper, optimization techniques were applied in *minG* (in order to simulate isothermal reactors) and *maxS* (in order to simulate adiabatic reactors) models to perform a complete thermodynamic characterization of different thermochemical routes. Pyrolysis (PR), Supercritical water gasification (SCWG), steam reforming (SR), oxidative reforming (OR) and autothermal reforming (ATR) are thermodynamic characterized aiming hydrogen production from LB with the aim of understand the thermal and reaction behavior of these complex systems.

## 2. Methodology

### 2.1. Isothermal reactors: formulation as a Gibbs energy minimization (*minG*) model

The equilibrium composition can be determined for a system with multiple components and phases, for a system at conditions of constant pressure and temperature, by direct *minG* of the system considering the number of moles of each component in each phase. Eq (1) represents this for a system considering the possible formation of a gas, a liquid and a solid phase (Freitas and Guirardello, 2014).

$$\min G = \sum_{i=1}^{NC} n_i^g \mu_i^g + \sum_{i=1}^{NC} n_i^l \mu_i^l + \sum_{i=1}^{NC} n_i^s \mu_i^s \quad (1)$$

The restrictions for the model are found in the non-negativity of the number of moles of each component in each phase and the balance of moles obtained by the atomic balance for reactive systems (Eq (2)).

$$\sum_{i=1}^{NC} a_{mi} (n_i^g + n_i^l + n_i^s) = \sum_{i=1}^{NC} a_{mi} n_i^0, \quad m = 1, \dots, NE, \quad n_i^g, n_i^l, n_i^s \geq 0 \quad (2)$$

The *minG* was calculated considering that the components were only on gaseous phase and there was only coke formation (represent as pure carbon) in solid phase. These considerations were used in previous research with good results (dos Santos et al., 2021). Eq (3) represents the Gibbs energy with these considerations.

$$G = \sum_{i=1}^{NC} n_i^g \left( \mu_i^g + RT(\ln P + \ln y_i + \ln \hat{\phi}_i) \right) + n_{c(s)} \mu_{c(s)} \quad (3)$$

Non-ideality was represented by the fugacity coefficient, calculated by truncated virial state equations in the second coefficient. The equation for the second virial coefficient was based on Pitzer's (Pitzer et al., 1955) correlation modified by Tsonopoulos (1974). The equation is shown as Eq (4). These combination of thermodynamic formulation and equation of state was used previously with good results for reforming systems as reported in Freitas and Guirardello (2014).

$$\ln \hat{\phi}_i = \left[ 2 \sum_j^m y_j B_{ij} - B \right] \frac{P}{RT} \quad (4)$$

### 2.2. Adiabatic reactors: formulation as an entropy maximization (*maxS*) model

Thermodynamic equilibrium can also be studied by maximizing the entropy of the system at constant pressure and enthalpy as presented in Eq (5).

$$\max S = \sum_{i=1}^{NC} n_i^g S_i^g + \sum_{i=1}^{NC} n_i^l S_i^l + \sum_{i=1}^{NC} n_i^s S_i^s \quad (5)$$

The restrictions for non-negativity of number of moles and atom balance (Eq (2)) are also necessary for the *maxS* model, with the conservation of enthalpy and the non-negativity of temperature, represented in Eq (6).

$$\sum_{i=1}^{NC} (n_i^g H_i^g + n_i^l H_i^l + n_i^s H_i^s) = \sum_{i=1}^{NC} n_i^0 H_i^0 = H^0, \quad T \geq 0 \quad (6)$$

In this model, the non-ideality of the vapor phase was also considered through the use of the virial equation, by calculating the fugacity coefficient through Eq (4). Both models are compared with experimental data from previous papers, with very good results (Freitas and Guirardello, 2014).

### 2.3. Thermodynamic analysis conditions

The models used perform simultaneous chemical and phase equilibrium calculations and are formulated as non-linear programming problems. To carry out the simulations, the GAMS (General Algebraic Modeling Systems) ® 23.9.5 software was used in combination with CONOPT3 solver. This solver is based on the concept of generalized reduced gradient, a reliable algorithm for solving non-linear programming problems, such as the *minG* and *maxS* methods proposed by the present work.

This combination of software and solver was previously used in previous works with excellent results (Gomes et al., 2022). LB was represented in simulations as a pseudocomponent with the following chemical formula:  $C_6H_{10}O_5$ . A total of 12 compounds were considered during simulations including: hydrogen ( $H_2$ ), methane ( $CH_4$ ), water ( $H_2O$ ), carbon monoxide ( $CO$ ), carbon dioxide ( $CO_2$ ), oxygen ( $O_2$ ), nitrogen ( $N_2$ ), ammonia ( $NH_3$ ), nitric oxide ( $NO$ ), nitrogen dioxide ( $NO_2$ ), methanol ( $CH_3OH$ ) and ethane ( $C_2H_6$ ). All thermodynamic properties of considered compounds were obtained in Polling et al. (2001). Thermodynamic models similar to the one developed and used in this work were previously validated with experimental data, showing excellent predictive capacity (Freitas and Guirardello, 2014). In this work the thermochemical routes of pyrolysis (PR), supercritical water gasification (SCWG), steam reforming (SR), oxidative reforming (OR) and autothermal reforming (ATR) aiming hydrogen production from LB were thermodynamic evaluated, effects of pressure and were evaluated as presented in Table 1. The feed composition was fixed for all simulations as presented in Table 1.

Table 1: reaction conditions analyzed for the studied thermochemical routes of LB.

Thermochemical route	Temperature (K)	Pressure (bar)	Feed composition (wt%)
Pyrolysis	800 - 1200	5 – 40	Only LB (100%)
Steam reforming	600 - 1000	1 – 10	15% LB and 85% $H_2O$
Supercritical water gasification	600 - 1000	230 – 280	3.5% LB and 96.5% $H_2O$
Oxidative reforming	500 - 900	1 – 10	15% LB and 85% $O_2$
Autothermal reforming	500 – 900	1 – 10	15% LB and 42.5% $H_2O$ and 42.5% $O_2$

### 3. Results and discussion

Figure 1 presents the results of the effect of temperature on isothermal and adiabatic systems for the five thermochemical processes evaluated. In Figure 1 (a) for the ATR reaction, in Figure 1 (b) for the PR reaction, in Figure 1 (c) for the OR reaction, in Figure 1 (d) for the SR reaction, and in Figure 1 (e) for the SCWG reaction. Analyzing the results presented on this figure, it can be seen that all processes showed significant differences in the molar quantity of  $H_2$  produced as a function of temperature and as a function of the way the reaction was conducted in reactor.

In general, it can be seen, by analyzing the results presented in Figure 1, that the ATR process showed higher productivity in  $H_2$  for adiabatic conditions up to a temperature of 700 K and for isothermal conditions above this temperature, this behavior is directly associated with the thermal behavior of this reaction. The PR process, with regard to the formation of  $H_2$ , was favored by isothermal operating conditions, especially at high operating temperatures. This behavior is also directly associated with the thermal characteristic of this process. The OR process had  $H_2$  formation behavior similar to that observed for ATR, although smaller molar amounts of  $H_2$  were produced, this result is explained by the reduction in the molar proportion of  $H_2$  atoms in the feed stream, due to the removal of  $H_2O$  from this stream. The SR process proved to be greatly favored by isothermal feeding conditions, increases in the order of 50% in the total molar production of  $H_2$  were observed at 900 K. The SCWG process showed similar behavior between the two routes (adiabatic and isothermic), with the largest molar productions of  $H_2$  observed at 1000 K in the adiabatic condition, here it is important to emphasize that the high amount in moles of  $H_2$  produced in this reaction, when compared with the other routes, is directly linked to the large excess of water used to feed this type of reactive system (see Table 1).

Figure 2 presents the results for the effect of the system's equilibrium temperature as a function of the initial reaction temperature. In Figure 2 (a) for the ATR reaction, in Figure 2 (b) for the PR reaction, in Figure 2 (c) for the OR reaction, in Figure 2 (d) for the SR reaction, and in Figure 2 (e) for the SCWG reaction. Analyzing the results, it is possible to verify that the ATR process, as expected, presents exothermic behavior, due to oxygen used as feed in this reactive system, the use of air was also tested and a slight reduction in equilibrium temperature was observed (in order of 7.5%) the  $N_2$  presented in air behaved mostly as an inert gas in the system, with only small amounts (traces) of  $NH_3$  and  $NO_x$  observed in the products. PR reaction presents endothermic behavior for the operating range of temperatures above 1000K, with a slightly exothermic general behavior being observed for lower temperatures, this behavior can be explained by the oxygen-rich molar composition of the lignocellulosic material used. The OR reaction, as well as the ATR, proved to be

exothermic within the entire range of temperature studied, here air was also tested as oxygen source too, it is important to report a slight reduction in the total amount of  $H_2$  produced when air was used, both for isothermal and adiabatic systems. These results are associated with the consumption of  $H_2$  to produce  $NH_3$  in isothermal systems and with a reduction in the equilibrium temperature for adiabatic systems. At high temperatures (above 900 K) SR was an endothermic reaction, being autothermal at a temperature of 900 K and slightly exothermic under higher temperatures. The SCWG reaction proved to be exothermic for almost the entire temperature range studied, being autothermal only at 1000 K (highest temperature tested).

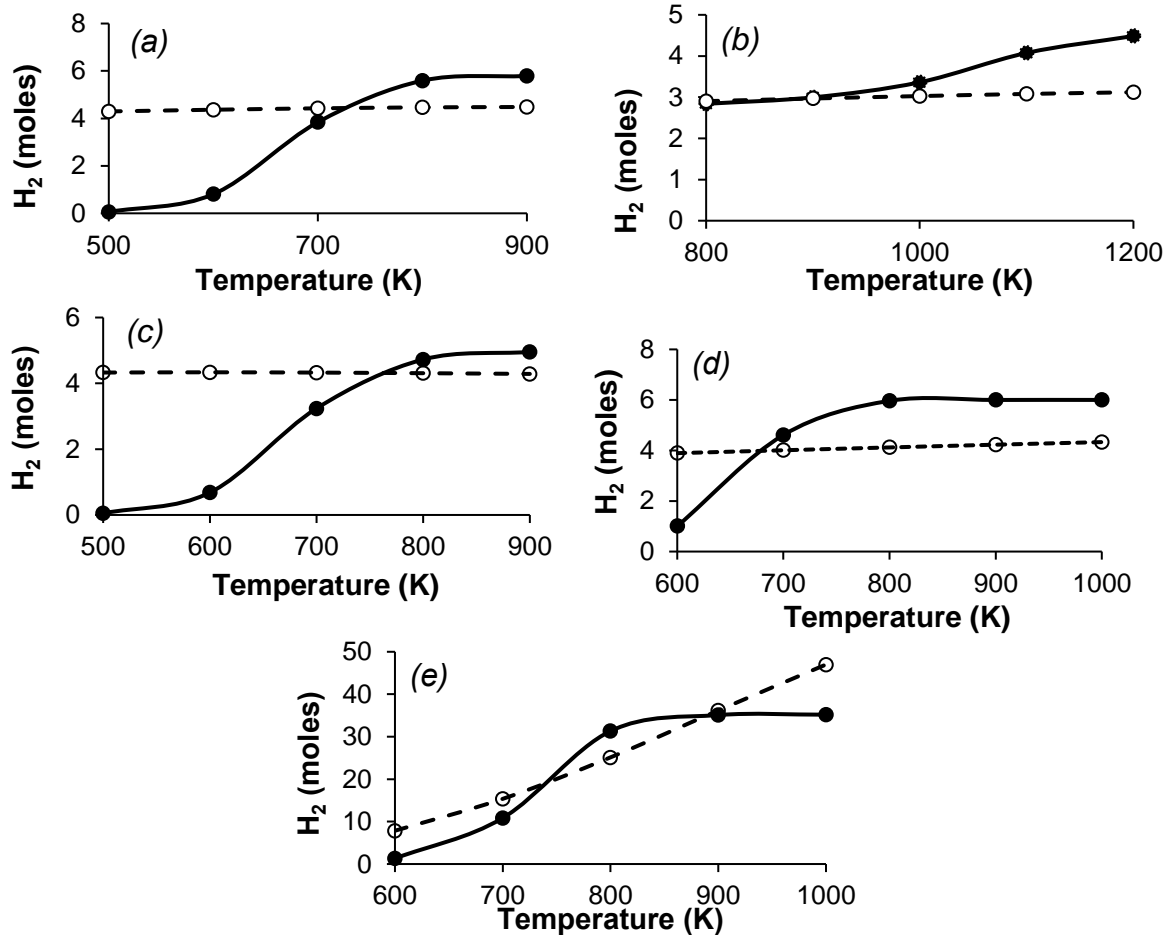


Figure 1: Hydrogen production in moles as function of temperature during (a) ATR, (b) PR, (c) OR, (d) SR and (e) SCWG reactions. Legend:  $\rightarrow$  isothermic reactors and  $\dashrightarrow$  adiabatic reactors. ATR, PR, OR and SR at 1 bar and SCWG at 230 bar.

Conflicting the results presented in Figures 1 and 2, it appears that the regions of greater molar production of  $H_2$  are associated with regions of higher temperatures of the reactive systems. This behavior is interesting, as it is an indication that the processes that lead to production of  $H_2$  in thermochemical conversion of LB systems are associated with reactions that require high temperatures, probably being linked to decomposition processes of LB. As a result, mostly exothermic processes have an operational advantage, by guaranteeing higher operational temperatures for the system and, consequently, higher  $H_2$  productions.

Figure 3 presents the results for the effect of pressure on the molar fraction of  $H_2$  in the systems studied. Here, the operating temperature was set at 800 K for all studied thermochemical processes. From this figure, it is possible to verify that the highest molar fractions of  $H_2$  in the product stream were observed under isothermal conditions, for the ATR (0.47) and SR (0.46) systems, both results being obtained under atmospheric pressure (lowest pressure considered in simulations). The OR and PR reactions showed behaviors where the adiabatic processes were more efficient in producing higher molar fractions of  $H_2$  in the product stream, with this behavior being observed across the entire pressure range for PR and at pressures above 3.0 bar for OR. The lowest molar fractions of  $H_2$  were observed for the SCWG process, although this process is responsible for the highest total molar production of  $H_2$  (as presented in Figure 1); this behavior can be explained by the excess water used to feed this system, which generates a dilution effect when considering

the total number of moles in the system. In dry basis all results are more similar for hydrogen, with the lowest  $H_2$  molar fraction observed in the PR reaction (average of 0.26 on a dry basis) and the highest  $H_2$  molar fraction observed in the SCWG reaction (average of 0.46 on a dry basis). The analysis of the results also shows that, within the evaluated reaction conditions, the reactor operating mode (adiabatic or isothermal operations) and the temperature in that the reaction was conducted have a greater influence on the  $H_2$  production behavior than the system operating pressure. Similar results are reported for thermochemical treatments of other carbonaceous materials (Freitas and Guirardello, 2013).

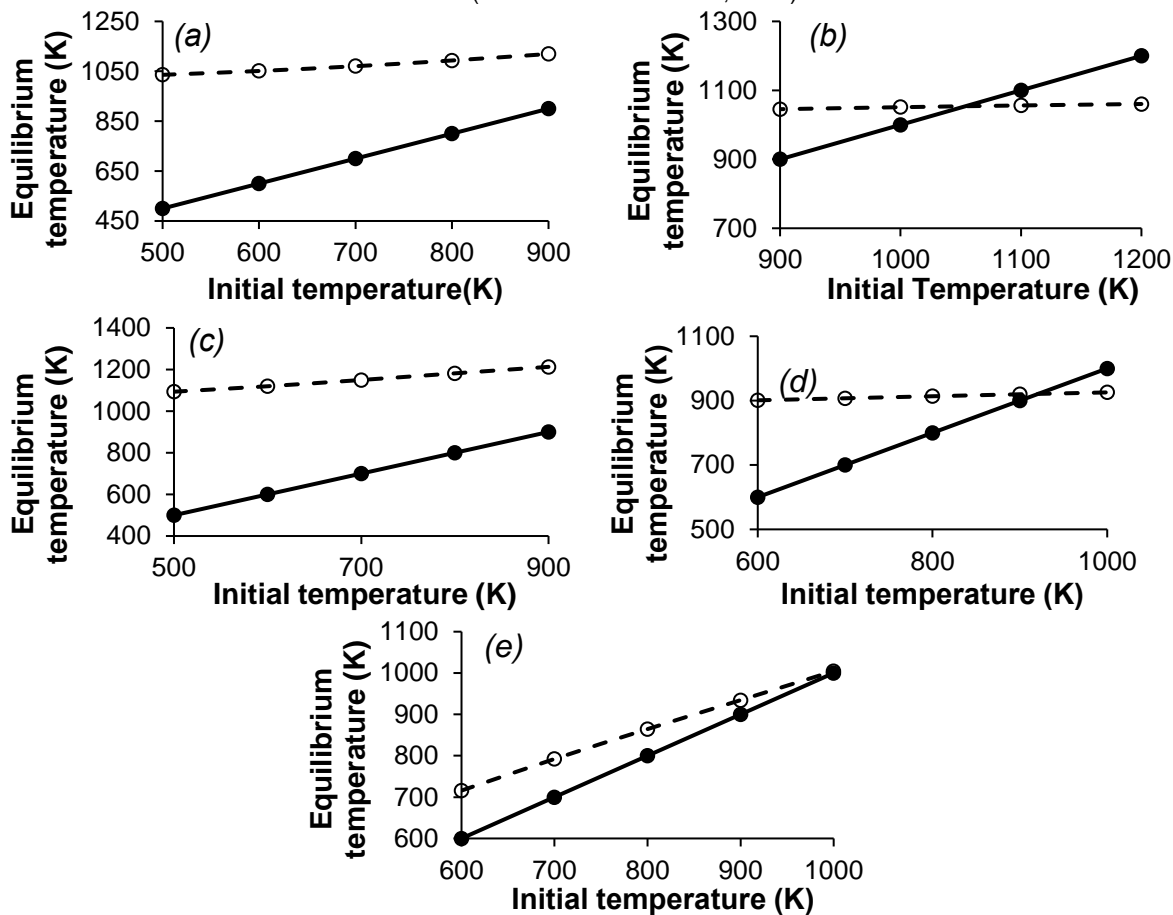


Figure 2. Equilibrium temperatures as function of initial temperature during (a) ATR, (b) PR, (c) OR, (d) SR and (e) SCWG reactions. Legend:  $\rightarrow$  isothermic reactors and  $-\cdot-$  adiabatic reactors. ATR, PR, OR and SR at 1 bar and SCWG at 230 bar.

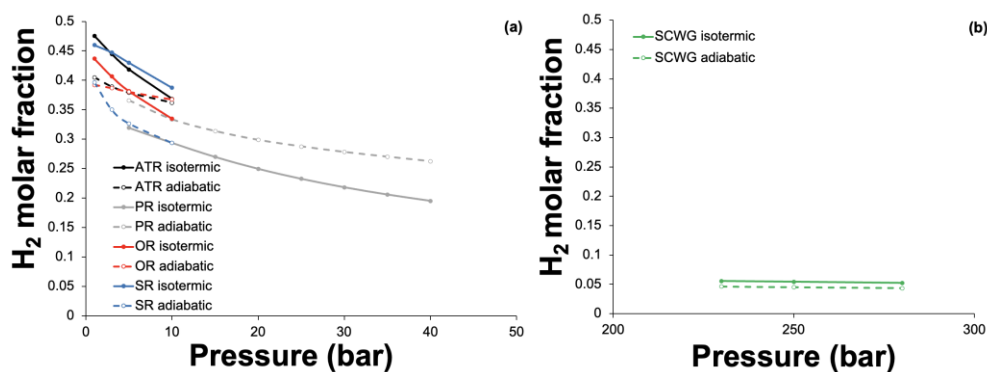


Figure 3. Effect of pressure for isothermic (solid lines) and adiabatic (dashed lines) reforming systems for the different thermochemical processes studied (a) ATR, PR, OR and SR processes and (b) SCWG process.

#### 4. Conclusion

The regions of maximum hydrogen production for each thermochemical route were evaluated using thermodynamic modelling considering isothermic and adiabatic operations throughout *minG* and *maxS* methods, respectively. The results showed that greater quantities of moles of hydrogen were produced in isothermal reactors for the SR, OR, ATR and PR routes. Only SWCG produce greater quantities of moles of hydrogen in an adiabatic system. Furthermore, the same trend was observed across all thermochemical routes for isothermal and adiabatic reactors: hydrogen productions were favoured at higher temperatures and lower operating pressures. It was also possible to verify that in terms of pressure effect, among the routes covered, SWCG was the route that presented the pressure parameter with the most discrete influence on hydrogen production. All routes were favoured in the production of hydrogen at a pressure of 1 bar, which was the lowest pressure tested by this work. As expected, due to the characteristics of the LB reactions, the increase in pressure resulted in a decrease in the production of hydrogen gas. However, the operational reactor condition (isothermic or adiabatic) and reactional temperature proved to be the most relevant factors for H<sub>2</sub> production. Both proposed thermodynamic models proved to be fast and effective in the calculations carried out in this paper, with computational times of less than 5 seconds in all performed simulations.

#### Nomenclature

$a_{mi}$  – Number of atoms of element  $i$  in component  $m$

$B$  – Second coefficient of the virial

$B_j$  – Second coefficient of the virial for mixture

$\phi_i$  – Fugacity coefficient of component  $i$

$\hat{\phi}_i$  – Fugacity coefficient of component  $i$  in mixture

$R$  – Universal gas Constant

$g$  – Gas phase

$G$  – Gibbs energy

$H_i^k$  – Enthalpy of component  $i$  in phase  $k$

$H_i^0$  – Enthalpy of component  $i$  in standard phase

$H^0$  – Total enthalpy

$l$  – Liquid phase

$T$  – Temperature

$P$  – Pressure

$s$  – Solid phase

$S_i^k$  – Entropy of component  $i$  in phase  $k$

$S_i^0$  – Entropy of component  $i$  in standard phase

$n_i^k$  – Number of moles of component  $i$  in phase  $k$

$n_i^0$  – Number of moles in standard phase

$NC$  – Number of components

$NE$  – Number of elements

$\mu_i^k$  – Chemical potential of component  $i$  in phase  $k$

$y_i$  – Molar fraction of gas phase

#### Acknowledgments

We are grateful for the financial support from the National Agency of Petroleum, Natural Gas and Biofuels (ANP) through the ANP Human Resources Training Program for the Oil and Gas Sector (PRH 54.1 - UFMA).

#### References

- Arregi, Aitor et al. Evaluation of thermochemical routes for hydrogen production from biomass: A review. *Energy conversion and management*, v. 165, p. 696-719, 2018.
- Dos Santos, J.M.; De Sousa, G.F.B.; Vidotti, A.D.S.; De Freitas, A.C.D.; Guirardello, R. Optimization of glycerol gasification process in supercritical water using thermodynamic approach. *Chemical Engineering Transactions*. 2021, 86, 847–852.
- Freitas, A.C.D.; Guirardello, R. Comparison of several glycerol reforming methods for hydrogen and syngas production using Gibbs energy minimization. *Int. J. Hydrogen Energy* 2014, 39, 17969–17984.
- Freitas, A. C. D.; Guirardello, R. Thermodynamic analysis of supercritical water gasification of microalgae biomass for hydrogen and syngas. *Chemical Engineering Transactions*, v. 32, p. 553-558, 2013.
- Gomes, J. G.; Mitoura, J.; Vidotti, A. D. S.; Freitas, A. C. D.; Guirardello, R. Analysis of Hydrogen Production from Glycerol Gasification using Supercritical and Subcritical Water. *Chemical Engineering Transactions*, v. 92, p. 133-139, 2022.
- Nanda, Sonil et al. Subcritical and supercritical water gasification of lignocellulosic biomass impregnated with nickel nanocatalyst for hydrogen production. *International Journal of Hydrogen Energy*, v. 41, n. 9, p. 4907-4921, 2016.
- Pitzer, K.S.; Lippmann, D.Z.; Curl, R.F.; Huggins, C.M.; Petersen, D.E. The Volumetric and Thermodynamic Properties of Fluids. II. Compressibility Factor, Vapor Pressure and Entropy of Vaporization. *J. Am. Chem. Soc.* 1955, 77, 3433–3440.
- Poling, B.E.; Prausnitz, J.M.; O'connell, J.P. *Properties of Gases and Liquids*; McGraw-Hill Education: New York, NY, USA, 2001.
- Tsonopoulos, C. An empirical correlation of second virial coefficients. *AIChE J.* 1974, 20, 263–272.
- Zabaniotou, A. et al. Experimental study of pyrolysis for potential energy, hydrogen and carbon material production from lignocellulosic biomass. *International Journal of Hydrogen Energy*, v. 33, n. 10, p. 2433-2444, 2008.